Experimental Parasitology 221 (2021) 108060

Contents lists available at ScienceDirect

Experimental Parasitology

journal homepage: www.elsevier.com/locate/yexpr

Differential expression of *Acanthamoeba castellanii* proteins during amoebic keratitis in rats

Ana Carolina Carvalho-Silva [a], Camila H. Coelho [b], Cecília Cirelli [a], Frederico Crepaldi [a], Isabela Aurora Rodrigues-Chagas [a], Cinthia Furst [c], Daniel Carvalho Pimenta [d], Juliano Simões de Toledo [a], Ana Paula Fernandes [a], Adriana Oliveira Costa [a,*]

[a] Department of Clinical and Toxicological Analysis, Federal University of Minas Gerais, Belo Horizonte, MG, Brazil
[b] Laboratory of Malaria Immunology and Vaccinology, National Institute of Allergy and Infectious Diseases, National Institutes of Health, Bethesda, MD, USA
[c] Department of Pathology, Health Sciences Center, Federal University of Espírito Santo, Vitória, ES, Brazil
[d] Biochemistry and Biophysics Laboratory, Butantan Institute, São Paulo, SP, Brazil

ARTICLE INFO

Keywords:
Acanthamoeba
Amoebic keratitis rat model
Proteomics

ABSTRACT

Amoebic keratitis (AK) is a sight-threatening infection characterized by a severe inflammation of the cornea, caused by the free-living protozoan of the genus *Acanthamoeba*. Identification of amoebic proteins involved in AK pathogenesis may help to elucidate molecular mechanisms of infection and contribute to indicate diagnostic and therapeutic targets. In this study, we evaluated changes in the expression profile of *Acanthamoeba* proteins triggered by the invasive process, using an approach involving two-dimensional polyacrylamide gel electrophoresis (2DE PAGE), followed by mass spectrometry identification (ESI-IT-TOF LC-MSn). AK was induced by intrastromal inoculation in Wistar rats, using trophozoites from a T4 genotype, human case-derived *A. castellanii* strain under prolonged axenic culture. Cultures re-isolated from the lesions after two successive passages in the animals were used as biological triplicate for proteomic experiments. Analysis of the protein profile comparing long-term and re-isolated cultures indicated 62 significant spots, from which 27 proteins could be identified in the *Acanthamoeba* proteome database. Five of them (Serpin, Carboxypeptidase A1, Hypothetical protein, Calponin domain-containing protein, aldo/keto reductase) were exclusively found in the re-isolated trophozoites. Our analysis also revealed that a concerted modulation of several biochemical pathways is triggered when *A. castellanii* switches from a free-living style to a parasitic mode, including energetic metabolism, proteolytic activity, control of gene expression, protein degradation and methylation of DNA, which may be also involved in gain of virulence in an animal model of AK.

1. Introduction

Amoebae are a group of widely diverse protozoa that includes some species capable of living primarily as free-living organisms and eventually as parasites (Visvesvara et al., 2007). Among such amphizoic amoeba, the most frequently found in the environment are those belonging to genus *Acanthamoeba* (Siddiqui et al., 2012).

Acanthamoeba species evoke clinical interest because they can cause two main severe infections in humans: granulomatous amoebic encephalitis (GAE) and amoebic keratitis (AK). GAE is a rare central nervous system (CNS) infection with more than 90% of lethality and predominantly associated with immunocompromised patients (Kalra et al., 2020; Siddiqui et al., 2012). AK is a sight-threatening infection of the cornea whose number of cases has been increasing in the last decades. Contact lenses users are considered the main risk group for developing AK, because of the susceptibility of the lens and other accessories to contamination and the occurrence of corneal micro-traumas predisposing to infection (Neelam and Niederkorn, 2017; Siddiqui et al., 2012) In many situations, the similarity of AK to another microbial keratitis delays the diagnosis, resulting in poor response to treatment and, sometimes, demanding corneal transplantation (Lorenzo-Morales et al., 2015; Siddiqui et al., 2012).

Interaction between human hosts and *Acanthamoeba* is a frequent event. The eventual parasitic behavior of *Acanthamoeba* depends on

* Corresponding author. Department of Clinical and Toxicological Analysis, Federal University of Minas Gerais, Av Pres. Antônio Carlos 6627, Belo Horizonte, MG, 31270-901, Brazil.
E-mail address: adrincosta@gmail.com (A.O. Costa).

https://doi.org/10.1016/j.exppara.2020.108060
Received 1 April 2020; Received in revised form 4 November 2020; Accepted 13 December 2020
Available online 15 December 2020

several factors, including the occurrence of specific genotypes. Twenty genotypes have been described (T1 to T20), but T4 is the most prevalent in the environment and human infections (Corsaro et al., 2015; Maciver et al., 2013). The expression of proteases is also considered an important factor associated with the pathogenicity of *Acanthamoeba*. Some proteases already characterized are the serine proteases of 33 kD, that exhibits activity against extracellular matrix (Kim et al., 2006) and MIP133, whose production is activated by contact with mannosylated glycoproteins of host cells (Clarke and Niederkorn, 2006; Garate et al., 2006; Neelam and Niederkorn, 2017). A key protein in MIP133 activation is a surface mannose-binding protein (MBP) that is largely expressed in strains that exert an intense cytopathic effect in host cells (Garate et al., 2006). Additional molecular classes of proteins identified as important in the *Acanthamoeba* invasive process are a pore-forming protein (Michalek et al., 2013) the laminin-binding protein (AhLBP) (Hong et al., 2004) and cysteine-proteases (Ramirez-Rico et al., 2015). The identification of additional proteins could provide a more complete understanding of the molecular mechanisms involved in the transition from free-living to parasitic life.

Proteomics is a promising approach to unveil the molecules involved in the pathophysiology of parasitic infection (Coelho et al., 2016). Regarding *Acanthamoeba*, previous studies using this approach have described a proteomic profile of trophozoites (Caumo et al., 2014), compared cysts and trophozoites stages (Behera and Satpathy, 2016), and investigated soluble and surface-enriched fractions of trophozoites (Maschio et al., 2018). Here, a comparative study was conducted to determine molecules involved in *A. castellanii* infection, using an *A. castellanii* in prolonged axenic culture and the correspondent isolate recovered from experimentally infected rat corneas. We hypothesize that this approach may unveil proteins that could be related to pathogenicity traits, which are induced by the direct contact of *Acanthamoeba* trophozoites with the rat cornea.

2. Materials and methods

2.1. Acanthamoeba strain

The strain of *A. castellanii* used in the experiments was originally isolated from a patient with amoebic keratitis. It was characterized as pathogenic and classified into genotype T4 (strain ALX) (Duarte et al., 2013). Subcultures was done every 15 days in PYG medium (protease peptone, yeast extract, and glucose) (Visvesvara and Balamuth, 1975) with 10% fetal bovine serum and 2 μg/mL of Enrofloxacin (Baytril® Bayer) at 30 °C, for 10 years. This culture was named ALXltc (long-term culture) to differentiate from those re-isolated from corneal lesions.

2.2. In vivo infection and re-isolation

Experimental infection procedures were approved by the Ethics Committee on the Use of Animals CEUA-UFMG under protocol 166/2014. Three 45-days old male Wistar rats were used for intra-stromal inoculation of ALXltc trophozoites in exponential growth (72h of culture), based in procedures previously described (Costa et al., 2017; Ren and Wu, 2010). Briefly, rats were anesthetized with ketamine (60 mg/kg) and xylazine (7.5 mg/kg), and then inoculated in the left cornea with 2 μL of suspension containing 10^4 *Acanthamoeba* trophozoites. A single animal presented lesion on the fourth day after inoculation. This rat was euthanized, and then both corneas were removed under aseptic conditions and washed twice in sterile PBS. A fragment of 2 mm of the lesion was inoculated into 2 mL of complete PYG medium for incubation at 30 °C degrees. After four subcultures, re-isolated trophozoites were used to infect six rats. On the fourth day post-infection, fragments of corneal lesions from animals that developed AK were transferred to PYG, as previously described, to obtain cultures for further proteomic analyses. The three re-isolated cultures were denominated ALXrec1, ALXrec2, ALXrec3. Fragments of right corneas inoculated with PBS were also cultivated in PYG to confirm the absence of *Acanthamoeba*.

2.3. Protein extraction and two-dimensional gel electrophoresis (2DE)

A total of 1.0×10^8 trophozoites from cultures ALXltc, ALXrec1, ALXrec2 ALXrec3, each in triplicate, were used for protein extraction. Cells in exponential growth (72 h) were harvested from cultures and washed three times in PBS pH 7.2, by centrifugation at 2000×*g* for 10 min. Cells were suspended in 1 mL of lysis buffer (Tris-HCl [25 mM], pH 7.2) and sonicated in an ice bath (25 Hz, 5 cycles of 30 s, with an interval of 1 min between pulses). Lysates were centrifuged at 10,000×*g*, for 15 min, at 4 °C and the proteins were precipitated for 2 h with trichloroacetic acid (10%). Precipitates were washed three times with ice-cold acetone by centrifugation at 1000×*g* for 1 min. The pellet was air-dried and solubilized overnight in 500 μL of isoelectric focusing buffer (urea [7M], thiourea [2M], CHAPS 4%, DTT [65 mM], 1,5% buffer IPG pH 4–7). Protein concentration was determined by the Bradford method and the quality of proteins was assessed by one-dimensional electrophoresis in 12% polyacrylamide gel (SDS-PAGE).

For the first dimension run, 900 μg of total protein extract was separated by isoelectric focusing (IEF). Strips of 13 cm with immobilized pH gradient (pH 4–7) were passively rehydrated with the cell extract sample in IEF buffer for 18 h. The IEF was performed in an Ettan IPGphor 3 system (GE HealthCare, United Kingdom) under the following conditions: 1 h 100 V (STP), 1 h 200 V gradient (GRD), 1h 500 V GRD, 1h 1000 V STP, 1h 2000 V STP, 1h 4000 V STP, 8000 V until accumulating 60,000 V. In the second dimension run, proteins were separated by molecular weight in homogeneous 15% polyacrylamide gels (SDS-PAGE). The strips were equilibrated for 15 min in equilibration buffer I (Tris-HCl [1.5 M] pH 8.8; urea [6 M]; glycerol 99.5%; SDS 2%, 0.5% bromophenol blue and DTT [130 mM]) then for an additional 15 min in equilibration buffer II (Tris-HCl [1.5 M] pH 8.8; urea [6 M]; glycerol 99.5%; SDS 2%, 0.5% bromophenol blue and iodoacetamide [135 mM]). The strips, as well as the molecular weight standard (Page Ruler Plus pre stained Protein Ladder Thermo Scientific, USA) were sealed with 0.5% agarose in electrophoresis buffer (Tris [250 mM]; glycine [1.92 M]; 1% SDS; 0,5% bromophenol blue). The runs were performed in protein electrophoresis buffer (Tris-HCl pH 8.3 [250 mM]; glycine [1.92M] and 1% SDS). Electrophoresis was performed at 20 mA per gel. Gels were stained with Colloidal Coomassie Blue G-250 and further scanned using the densitometer Image Scanner III (GE HealthCare), calibrated with Kodak tablet n° 3. Gels were then stored at 4 °C, in ammonium sulfate [10%] until spot excision for mass spectrometry.

2.4. Analyses of 2DE gels images

The triplicates of gels 2DE from each group (ALXltc, ALXrec1, ALXrec2, ALXrec3) were analyzed by ImageMaster 2D Platinum 7 (GE HealthCare) using 5 pixels for minimum area, smooth factor of 2 and salience of 250 as parameters to detect the spots. All spots detected by the software were also confirmed manually. Gel images were processed using algorithms developed to detect, assign isoelectric point (pI) and molecular weight and to quantify and identify the corresponding spots between the sets of gels (match among triplicates). The reproducibility of the gels was assessed by scatter plots comparing the gels of each triplicate technique. ANOVA test ($p < 0.05$) was applied to detected differentially expressed protein between the samples.

2.5. Spots treatment and mass spectrometry

The spots of interest were manually excised from the gel and transferred to microcentrifuge tubes. For removal of blue stain, the spots were washed in a solution of ethanol 40% and ammonium bicarbonate [75 mM] pH 8.0. Acetonitrile (200 μL) was added for 5 min to dehydrate the gels. After dehydration, acetonitrile was removed and the gels were dried in a Speed Vac. Afterwards, the spots were trypsin [20 μg/mL]

treated with Sequencing Grade Modified Trypsin (Promega) and then a solution of ammonium bicarbonate ([25 mM] pH 8.0) were added. Samples were incubated for 16 h at 37 °C. After this time, the supernatant was transferred to a new tube, a solution of 5% formic acid and 50% acetonitrile was added to the tubes containing the gel fragment and incubated for 30 min with shaking to increase the recovery of tryptic peptides. This procedure was performed twice more, and the supernatants were transferred to the original tube. Samples were completely dried in SpeedVac and sent for mass spectrometry analyses at the Biochemistry and Biophysics Laboratory, Butantan Institute in São Paulo, Brazil.

The peptides were loaded onto a C18 column (Supelco, 2.1 × 50 mm, 100 Å) coupled to a Shimadzu ESI-IT-TOF LC-MSn system (Shimadzu Co., Japan). A linear gradient from 0 to 40% solvent B1 (A1: 0.1% AA; B1: 90% ACN containing 0.1% AA) was used to elute the peptides. The main parameters of the instrument were 4.5 kV interface voltage, 1.76 kV detector voltage and 200 °C capillary temperature, in a positive ionization mode, in a full scan mode (50–2000 m/z) followed by data dependent acquisition (DDA) MS2, a range of 100–2000 m/z obtained after ICD (Ar) fragmentation. Data acquisition and processing were performed by LC-MS Solutions software (Shimadzu Co, Japan). For protein identification, the processed spectra were analyzed by MASCOT (Matrix Science Inc) using MS/MS ion search mode, with 0.5 Da tolerance for MS and MS/MS and manually checked for accuracy and correctness. The complete NCBInr (Non-redundant RefSeq proteins) and *Acanthamoeba* subset databases were selected for research.

2.6. Data analysis

After identification, differentially expressed proteins were clustered by gene ontology (GO) categories and a heatmap and hierarchical clustering analysis (HCA) was plotted using the R software package *ggplot* with the script heatmap.2 (R x 64 3.1.3). Fold change was calculated based on the percentage volume displayed by each spot and comparing the pairs ALXrec1 X ALXltc, ALXrec2 X ALXltc and ALXrec3 X ALXltc. Fold change values were normalized in logarithm of base 2 (log_2).

3. Results

3.1. In vivo infection

The first attempt to induce AK in rats using trophozoites in prolonged axenic culture (ALXltc) resulted in a small, punctiform corneal lesion (1 mm in diameter) in only one out the three infected animals, suggesting an attenuated virulence profile, as expected. The re-isolated culture that was subsequently inoculated in six animals caused AK in three rats. The lesions measured 2–6 mm in diameter and were characterized by whitish areas, showing the typical inflammatory infiltrate of AK (Fig. 1B–D). Three independent cultures (ALXrec1, ALXrec2, ALXrec3) derived from these lesions, provided the trophozoites that constituted the biological triplicates for the proteomic experiments. All corneal fragments from rats inoculated with PBS as control rendered negative for *Acanthamoeba*. Fig. 1A shows the normal aspect of a right cornea inoculated with PBS.

3.2. Analysis of two-dimensional gels images

Trophozoites protein extracts of each *Acanthamoeba* culture, including the long-term and recovered from corneal lesions, were analyzed by 2DE proteomics. The protein profile indicated the predominance of spots in a range of pH 6 to 7, with molecular weight varying between 15 and 100 kDa (Supplementary Fig. S1).

Reproducibility was high among gel triplicates (Supplementary

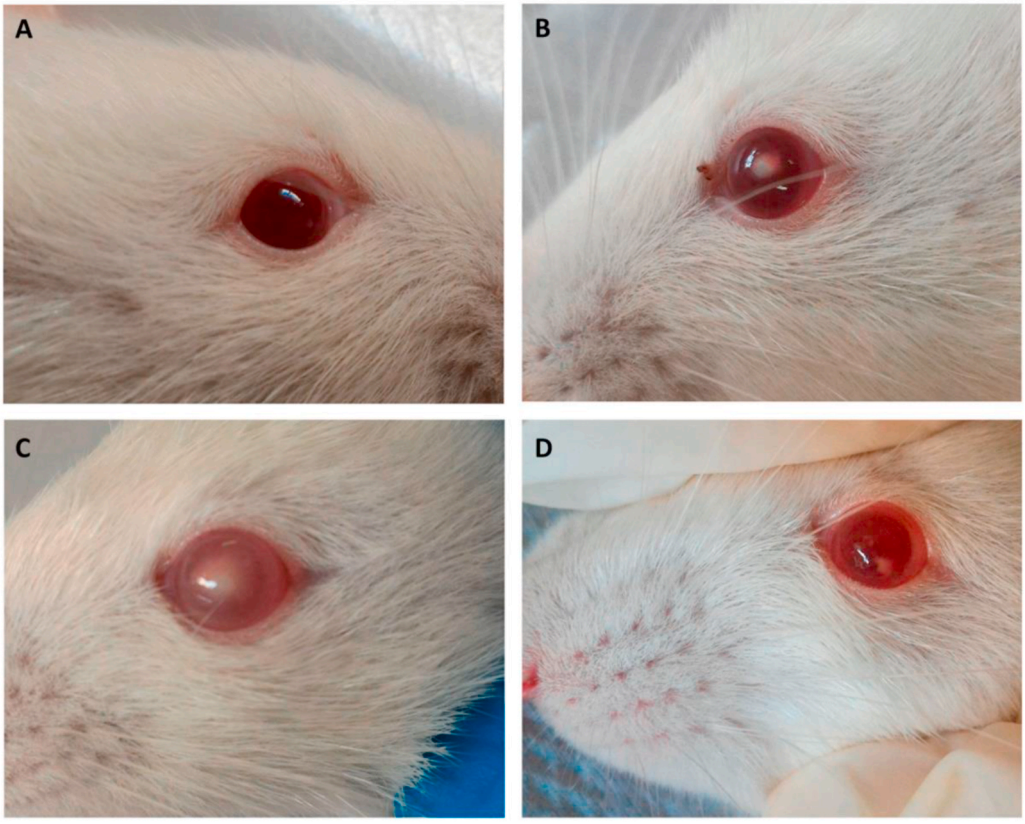

Fig. 1. *Acanthamoeba* keratitis induced in Wistar rats. A: Normal aspect of cornea inoculated with PBS. B–D: Ring-shaped inflammatory infiltrate in cornea of animals infected with *A. castellanii* by intra-stromal inoculation of 10^4 trophozoites.

Fig. S2), as indicated by percentages of matches from 50% to 89% (Supplementary Table S1). Scatter plot analysis confirmed the reproducibility of triplicate gels, with a coefficient of variation values from 0.83 to 0.96 (Supplementary Fig. S3).

3.3. Comparative analyses between long-term and re-isolated trophozoites

To identify the proteins differentially expressed in long-term and re-isolated cultures, the gels were matched to indicate the significant spots, as represented in Fig. 2.

A total of 62 significant spots ($p < 0.05$, One Way ANOVA) were sent for identification by ESI-IT-TOF LC-MSn. The spots were selected based on concomitant identification in at least two gels from the technical triplicates. Of these, 27 proteins were identified in *A. castellanii* proteome database (Supplementary Table S2), being 22 of those differentially expressed in long-term and re-isolated cultures (Table 1). Five proteins were found exclusively in the re-isolated cultures (Fig. 2 B), being three simultaneously detected in ALXrec1, ALXrec2, and ALXrec3 cultures (Fig. 3, Table 2).

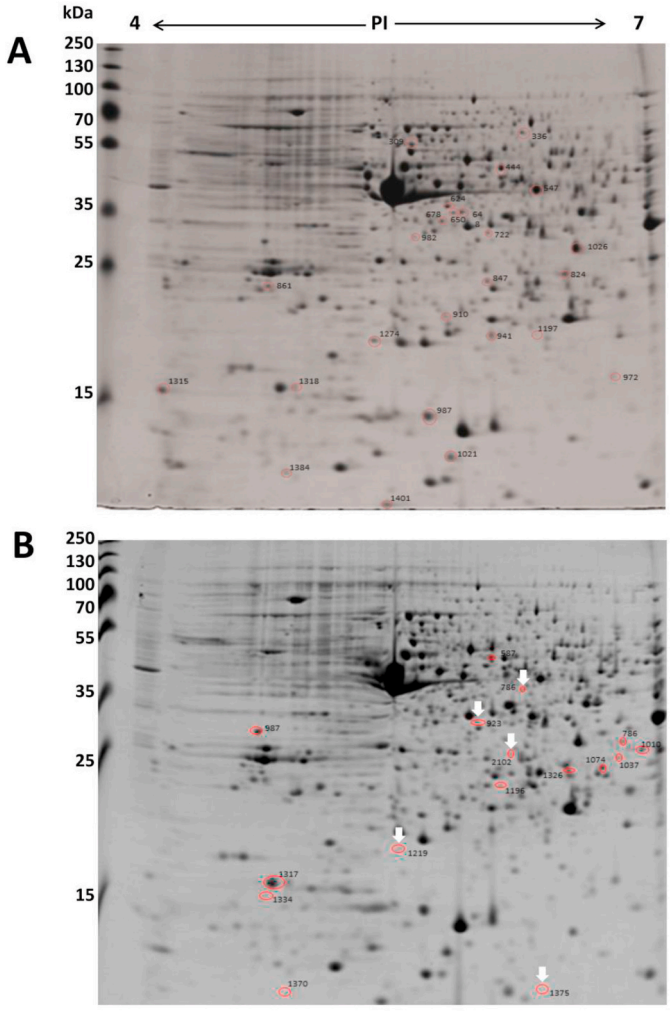

Fig. 2. Representative proteome of *Acanthamoeba castellanii* in long-term culture (A) and re-isolated from the cornea of a rat with *Acanthamoeba* keratitis (B). The proteins were separated on a linear pH range of 4–7, using IEF in the first dimension and 15% SDS-PAGE in the second dimension. Proteins were stained with Coomassie Blue G-250. Molecular mass markers are on the left, and the acid-to-alkaline gradient is displayed horizontally. Indicative numbers in the gel corresponding to the long-term culture (A) identify proteins listed in the Supplementary Table 2. Proteins found exclusively in re-isolated culture are indicated by white arrows in the gel B and listed in Table 2.

To differentiate expression levels among proteins from long-term and re-isolated cultures, fold change was calculated based on the percentage volume displayed by each spot, comparing the pairs ALXrec1 X ALXltc, ALXrec2 X ALXltc, and ALXrec3 X ALXltc. The raw data were normalized in each column by z-score. Analysis values were given to each spot through densitometry, allowing protein classification into three main clusters (Fig. 4). Eight proteins (fold change between 0 and 2) composed the upregulated cluster in re-isolated cultures: Ankyrin repeat-containing protein, Deoxyribosephosphate aldolase 1, Deoxyribosephosphate aldolase 2, Deoxyribosephosphate aldolase 3, Eukaryotic translation initiation factor 5A, Isochorismatase hydrolase, Superoxide dismutase [Cu–Zn], and Ubiquitin carboxyl-terminal hydrolase.

The second cluster included ten proteins with a discrete down-regulation (fold change entre −1 and 1) in re-isolated cultures compared to the long-term: Epithiospecifier protein fragment, Guanine nucleotide-binding protein beta subunit, putative, Inositol3-phosphate synthase, Rho guanine dissociation factor isoform 2, putative, Saccharopine dehydrogenase, S-adenosylmethionine synthase, Short/branched chain specific acylCoA dehydrogenase, mitochondrial, putative, Universal stress domain containing protein, Zinc binding dehydrogenase family oxidoreductase 1, Zinc binding dehydrogenase family oxidoreductase 2.

The third cluster contained six proteins presenting negative expression profiles of ALXrec lines compared to long-term, with fold changes between 0 and -2: 26S proteasome regulatory complex subunit RPN11, DNA repair protein RAD51, FAD binding domain containing protein, S-formylglutathione hydrolase, Hypothetical protein, Actin binding protein (ADF/cofilin family group). The protein Thiamine phosphate pyrophosphorylase presented a unique regulation pattern that separated it from the other groups (fold change between −1.8 and 1.8) (Fig. 4).

The proteins differentially expressed were grouped according to their molecular function and biological process annotated in the gene ontology (GO) (Supplementary Table 2). Most proteins have the molecular function of protein binding (18.8%) and participated in the process of oxidation-reduction (20.69%) (Fig. 5). Nine proteins did not present GO for Biological Processes. Four proteins did not present Molecular Function in *Acanthamoeba*, but they had annotation in *Entamoeba histolytica*, *Entamoeba dispar*, *Entamoeba invadens*, and *Plasmodium falciparum* databases (Supplementary Table 2).

4. Discussion

In this study, we compared the proteome of *A. castellanii* trophozoites recovered from corneal lesions induced in rats with those from prolonged axenic culture. Previous studies have already shown that the prolonged axenic culture attenuates the virulence properties of *Acanthamoeba*, and conversely, these properties could be restored after passages in animals (Mazur and Hadas, 1994; Verissimo et al., 2013). While such studies involved the animal models of systemic and encephalic acanthamoebiasis, we unprecedentedly used the AK model, which also resulted in an augmented virulence profile in re-isolated cultures.

In the proteomic analysis, cultures reactivated by two successive passages in AK animal model were used. Some proteins were identified only in these samples compared to the long-term trophozoites. Among these proteins exclusively found in re-isolated samples, the most expressed was Carboxypeptidase A1, a metalloprotease that exhibits proteolytic activity on components from the membrane and extracellular matrix (Itoh, 2002). In herpetic keratitis, several matrix metalloproteases are involved in the destruction of corneal tissue (Yang et al., 2003). This class of proteases can also act as a possible factor of pathogenicity in *Acanthamoeba* since they are also found in the repertory of proteases released by trophozoites (Alsam et al., 2005; Cao et al., 1998; Sissons et al., 2006). Thus, the detection of Carboxypeptidase A1 in rat recovered cultures but not in long-term cultures, reinforces the involvement of metalloproteases in *Acanthamoeba* pathogeny.

Table 1
Proteins identified in *Acanthamoeba castellanii* trophozoites from long-term culture and cultures recovered from rat corneal lesion.

Spot	Protein	Access number	exp. PI	theor. PI	exp. MM	theor. MM	Score	p value (ANOVA)
309	Inositol3-phosphate synthase	ACA1_058810	3.91	5.26	54.83	57.80	223	0.0293
336	FAD binding domain containing protein	ACA1_080550	6.28	5.97	62	66.4	145	0.0377
444	Saccharopine dehydrogenase	ACA1_310610	6.14	6.15	46.67	50.53	210	0.0136
547	S-adenosylmethionine synthase	ACA1_091670	6.37	6.37	40.67	42.85	416	0.0074
624	Short/branched chain specific acylCoA dehydrogenase, mitochondrial, putative	ACA1_384630	5.83	7.67	37	45.6	206	0.0378
648	Zinc binding dehydrogenase family oxidoreductase	ACA1_314990	4.12	6.16	35	38.50	95	0.0268
650	Zinc binding dehydrogenase family oxidoreductase	ACA1_314990	5.85	6.16	34.83	38.50	99	0.0028
678	DNA repair protein RAD51, putative	ACA1_201650	3.71	5.51	34.6	37.51	182	0.0498
722	26S proteasome regulatory complex subunit RPN11, putative	ACA1_073080	4.71	6.24	32.5	35.03	61	0.0120
824	S-formylglutathione hydrolase	ACA1_264380	5.54	6.56	24.67	31.51	102	0.0330
847	Universal stress domain containing protein	ACA1_368860	6.00	6.57	23	26.64	138	0.0025
861	Ubiquitin carboxyl-terminal hydrolase	ACA1_378160	3.04	4.38	23.2	26.78	53	0.0441
910	Hypothetical protein	ACA1_245960	5.80	10.18	21.3	14.65	32	0.0539
941	Rho guanine dissociation factor isoform 2, putative	ACA1_174240	5.17	6.06	19.5	22.87	180	0.0535
972	Thiaminephosphatepyrophosphorylase	ACA1_061790	4.32	6.93	16.2	48.71	34	0.028
982	Epithiospecifier protein (Fragment)	ACA1_198360	5.62	6.4	30.83	37.51	83	0.0037
997	Superoxide dismutase [Cu–Zn]	ACA1_048530	5.70	6.76	14.50	16.48	396	0.0191
1021	Actin binding protein (ADF/cofilin family group)	ACA1_035360	4.93	7.72	12.5	14.46	88	0.0504
1026	Guanine nucleotide-binding protein beta subunit, putative	ACA1_199990	6.60	6.48	28.83	35.54	611	0.00004
1197	Deoxyribosephosphate aldolase	ACA1_296270	6.32	4.8	19.2	43.17	51	0.03357
1274	Isochorismatase hydrolase	ACA1_384860	5.39	5.27	19.33	20	118	0.0340
1315	Eukaryotic translation initiation factor 5A	ACA1_023810	4.11	4.84	15.83	16.80	87	0.0069
1318	Deoxyribosephosphate aldolase	ACA1_296270	4.93	4.8	16.17	43.17	35	0.0316
1384	Deoxyribosephosphate aldolase	ACA1_296270	4.13	4.8	11.5	43.17	47	0.0035
1401	Ankyrin repeat containing protein	ACA1_391670	5.45	5.61	10.17	13.23	256	0.0040

exp. PI = Isoelectric point experimental; theor. PI = Isoelectric point theoretical; exp. MM = Molecular mass experimental; theor. MM = Molecular mass theoretical. Differences in expression levels are shown at Fig. 4.

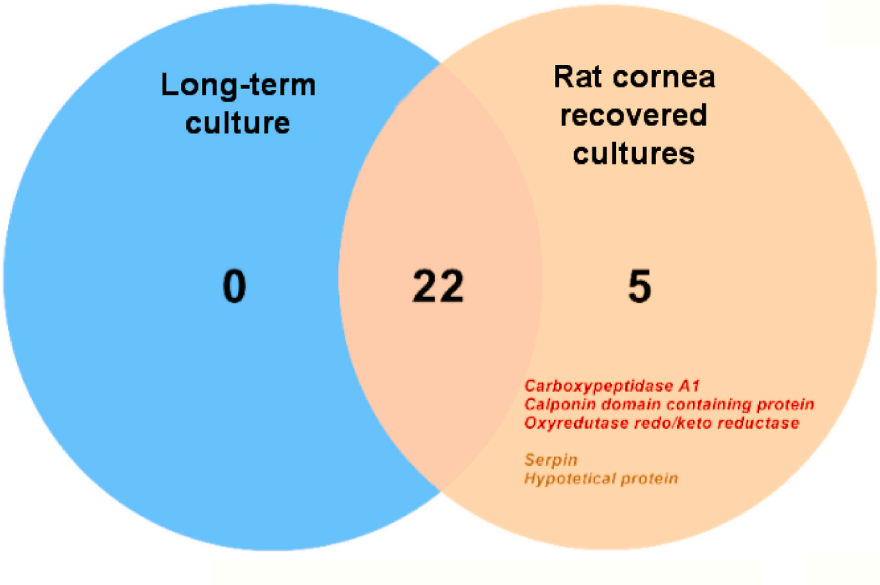

Fig. 3. Number of *Acanthamoeba castellanii* proteins identified in long-term culture and cultures re-isolated from corneal lesions of rats. Five proteins were identified only in the re-isolated cultures, while 22 proteins were identified in both long-term and re-isolated cultures. Proteins highlighted in red were identified in all of the three re-isolated cultures. (For interpretation of the references to color in this figure legend, the reader is referred to the Web version of this article.)

Another protein found exclusively and in high levels in the tissue-recovered cultures was the serine protease inhibitor (serpin). Serpin superfamily protein was previously described only in the *Acanthamoeba* genome, but a recent study identified it in a surface-enriched protein fraction of *Acanthamoeba* (Maschio et al., 2018). Intriguingly, serpin inhibits serine proteases (James, 1985), which in turn are important in the AK invasive process (Clarke and Niederkorn, 2006; Kong et al., 2000). Serpins are also described as a virulence factor in viruses. In the infection with Myxoma virus, Serp 1 acts inhibiting molecules involved in the modulation of the inflammatory response; Serp 2 presents anti-inflammatory action and can interfere with cell apoptosis (Guerin et al., 2001; Moon et al., 1999). Taking into account these findings, we suggest that serpin may have a potential role in the modulation of inflammatory responses during the invasive process.

Calponin domain containing protein was also identified exclusively in rat recovered cultures. Calponin is an actin-binding protein associated

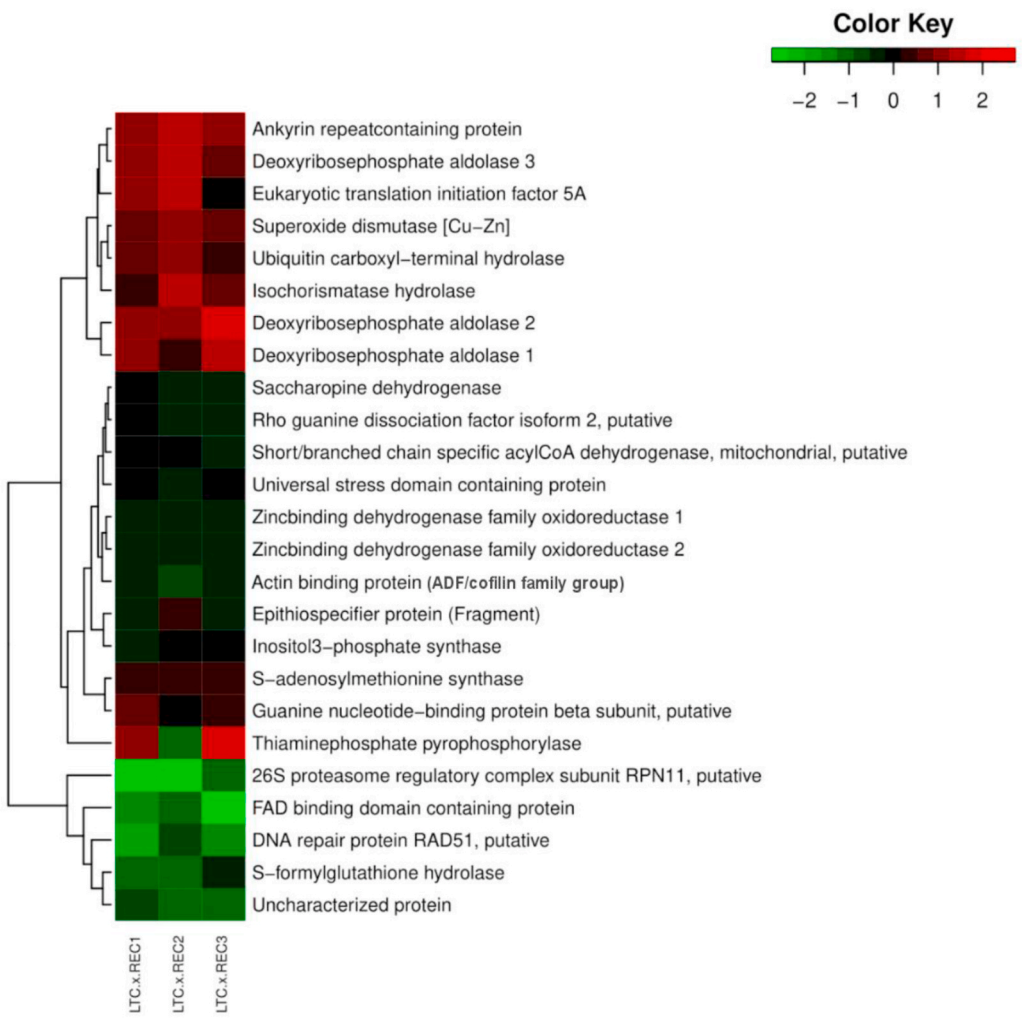

Fig. 4. Quantitative representation of proteins differentially expressed in *Acanthamoeba castellanii* from long-term culture (ALXltc) and cultures recovered from corneal lesion of rats (ALXrec1, ALXrec2, ALXrec3). The proteins identified by ESI-IT-TOF LC-MSn were organized in a heatmap displaying fold change pattern for each protein. Protein expression was analyzed by One Way ANOVA ($p < 0.05$). Fold change was calculated based on the percentage of volume displayed by each spot. The figure shows values of expression that varied between −2.0 (green) and 2.0 (red), indicating down-regulation and upregulation, respectively, of proteins from recovered cultures in relation to long-term one. Non-expressive fold changes (values next to zero) are shown in black. Normalized data and the heatmap were generated using R x 64 3.1.3 software utilizing scripts *ggplot/heatmap2*. (For interpretation of the references to color in this figure legend, the reader is referred to the Web version of this article.)

Table 2
Proteins of *Acanthamoeba castellanii* exclusively expressed in trophozoites recovered from corneal lesion in rat in comparison to the long-term culture.

Spot	Protein	Accession number	exp. IP	theor. IP	exp. MM	theor. MM	Score	p value (ANOVA)	Culture		
									ALX rec1	ALX rec2	ALX rec3
786	Serpin (Serine proteinase inhibitor) superfamily protein	ACA1_382620	6.22	6.19	36	40.24	44	0.0010	+	–	+
923	Carboxypeptidase A1, putative	ACA1_399750	5.95	6.01	30	47.68	73	0.00001	+	+	+
1219	Hypothetical protein	ACA1_097160	5.55	5.19	17.70	19.37	47	0.000008	+	+	+
1375	Calponin domain containing protein	ACA1_109720	3.93	6.93	11.86	48.94	97	0.0496	+	+	+
2102	Oxidoreductase, aldo/keto reductase, putative	ACA1_050180	4.31	6.05	25	34.38	72	0.0010	–	–	+

exp. PI = Isoelectric point experimental; theor. PI = Isoelectric point theoretical; exp. MM = Molecular mass experimental; theor. MM = Molecular mass theoretical; + and – represent presence or absence in each culture recovered from corneal lesion.

with smooth muscle contraction in the vertebrates (el-Mezgueldi, 1996). It has not been previously described either in the genome or as a protein expressed in *Acanthamoeba*. In *Entamoeba histolytica*, however, this protein appears in excretory-secretory products of trophozoites, presenting a higher level of expression in a virulent strain compared to a non-virulent (Ahn et al., 2018). Also, an actin-binding protein G (AbpG), whose structure presents a calponin homology domain, is associated with cell locomotion in the slime mold *Dictyostelium discoideum* (Lin et al., 2015). During the invasive process in *Acanthamoeba*, the actin cytoskeleton is involved in the locomotion and adhesion of trophozoites to host cells, which is consequently associated with the cytopathic effect (Gonzalez-Robles et al., 2008; Soto-Arredondo et al., 2014) Thus, as an actin-binding component, the calponin domain-containing protein may have a function in *Acanthamoeba* cytoskeleton arrangements and could then contribute to the establishment of infection.

An additional protein found exclusively in recovered cultures is Aldo-keto reductase, an enzymatic protein that reduces carbonyl substracts and is found in prokaryotic and eukaryotic domains of life (Penning, 2015). Aldo-keto reductase has not been previously described in *Acanthamoeba*, but it has been studied as a component involved in the drug metabolism of *Trypanosoma cruzi* (Garavaglia et al., 2016; Trochine et al., 2014). The exact role of Aldo-keto reductase in the context of

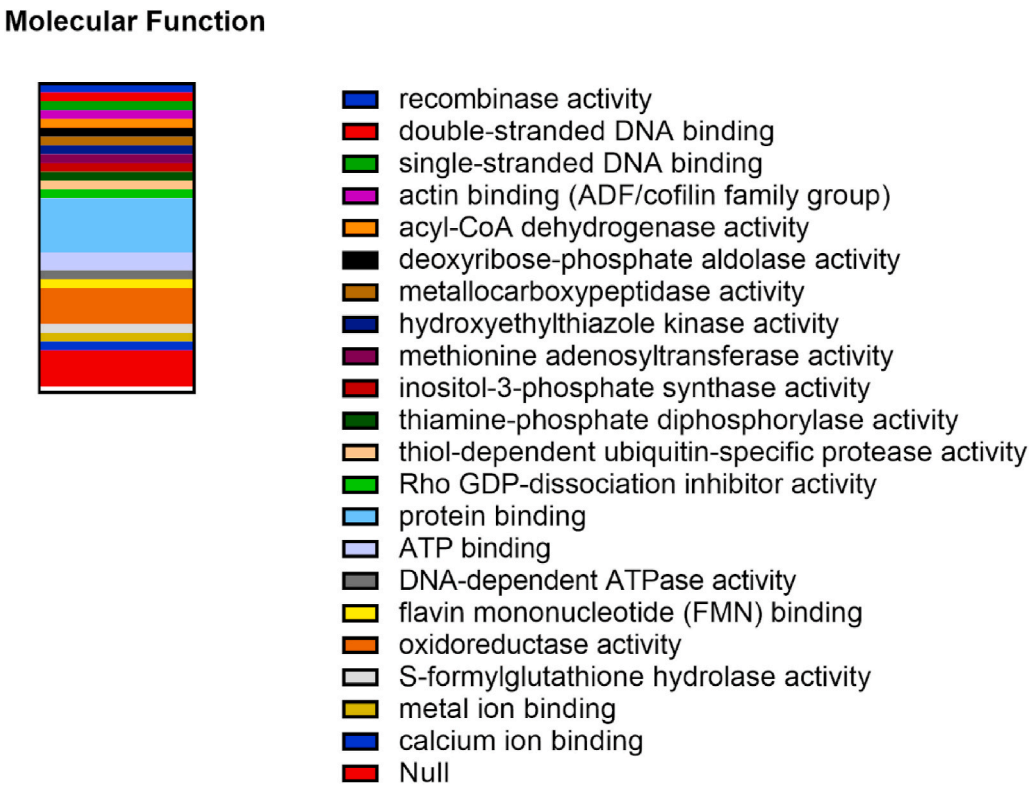

Fig. 5. Characterization of Molecular function and Biological processes of proteins differentially and exclusively expressed in long-term culture of *Acanthamoeba castellannii* (ALXltc) and cultures recovered from corneal lesion of rats (ALXrec1, ALXrec2 and ALXrec3). Based on functional annotations in Gene Ontology, proteins were distributed in different categories. Those with no annotation for Molecular function and Biological process in Gene Ontology for *Acanthamoeba* were categorized as Null. For Biological processes, twenty-nine categories of GO were associated with proteins. (For interpretation of the references to color in this figure legend, the reader is referred to the Web version of this article).

Acanthamoeba infection remains a point for further investigation.

Among the proteins found in both re-isolated and long-term culture, most of those up-regulated in the tissue-recovered samples were enzymes associated with metabolism, as Deoxyribosephosphate aldolases, Isochorismatase hydrolase, Superoxide dismutase [Cu–Zn] and Ubiquitin carboxyl-terminal hydrolase. Aldolases are involved in glycolytic pathways of the intestinal parasite *Giardia lamblia* (Galkin et al., 2007), and hydrolases participate in the pathogenic events during the *Acanthamoeba* and *Entamoeba histolytica* infection (Betanzos et al., 2019). Particularly important in the pathogeny of amoebic keratitis, hydrolases are required for demyelination and lysis of nerve cells (Betanzos et al., 2019). An adaptation of the metabolism resulting from contact with the

host organism can also explain the increased expression of these enzymes. Concerning the up-regulation of Superoxide dismutase [Cu–Zn], it could be a response to the oxidative burst triggered by inflammatory events during the infection, since it constitutes a cytosolic enzyme associated to protective mechanisms against superoxide radicals from defense cells (Broxton and Culotta, 2016; Fridovich, 1995).

Another up-regulated protein in the tissue-recovered cultures was Ubiquitin carboxyl-terminal hydrolase, a cysteine protease whose molecular function corresponds to the specific thiol-dependent protease in *Acanthamoeba*. This type of hydrolase is a deubiquitinating enzyme that cleaves monomers of ubiquitin-conjugate substrates. As a result, they have an antagonistic action on ubiquitin proteins, which leads to the degradation of other proteins and peptides (Amerik et al., 2006; Dirac et al., 2005; Nijman et al., 2005). On the other hand, another protein related to deubiquitination was found down-regulated in the tissue-recovered isolates. The regulatory complex 26S proteasome subunit RPN11 was the less expressed protein in the re-isolated trophozoites compared to those from the long-term culture (Amerik and Hochstrasser, 2004). In *Acanthamoeba*, this protein is annotated for the molecular function of binding to another protein, which can suggest that deubiquitination is necessary for the pathogenic process of *Acanthamoeba* in the cornea.

In this study, an animal model of AK was used to reactivate the virulence of *Acanthamoeba* trophozoites and identify proteins related to the invasive process. Our findings suggested that *Acanthamoeba* significantly modulates the expression of several proteins during their interaction with the host in the AK context.

Funding

This work was supported by grants from the Fundação de Amparo à Pesquisa do Estado de Minas Gerais-FAPEMIG, APQ-01100-14 and red001214 through Rede Mineira de Biomoléculas; Conselho Nacional de Desenvolvimento Científico e Tecnológico-CNPq, 406385/2018-1, and 465293/2014-0 through Instituto Nacional de Ciência e Tecnologia em Vacinas – INCTv; Financiadora de Estudos e Projetos-FINEP, 01.09.0278.04 and 01.12.0450.03. CHC is supported by the Intramural Research Program of the National Institute of Allergy and Infectious Diseases, IARC is supported by Coordenação de Aperfeiçoamento de Pessoal de Nível Superior-CAPES (finance code 001), and DCP is a CNPq fellow researcher (303792/2016-7).

CRediT authorship contribution statement

Ana Carolina Carvalho-Silva: Investigation, Formal analysis, Writing - original draft, Writing - review & editing. **Camila H. Coelho:** Investigation, Formal analysis, Visualization, Writing - review & editing. **Cecília Cirelli:** Investigation. **Frederico Crepaldi:** Investigation, Formal analysis. **Isabela Aurora Rodrigues-Chagas:** Investigation. **Cinthia Furst:** Investigation, Resources. **Daniel Carvalho Pimenta:** Formal analysis, Resources. **Juliano Simões de Toledo:** Supervision, Investigation, Visualization. **Ana Paula Fernandes:** Conceptualization, Supervision, Funding acquisition. **Adriana Oliveira Costa:** Conceptualization, Project administration, Funding acquisition, Writing - review & editing.

Declaration of competing interest

None.

Appendix A. Supplementary data

Supplementary data to this article can be found online at https://doi.org/10.1016/j.exppara.2020.108060.

References

Ahn, C.S., Kim, J.G., Shin, M.H., Lee, Y.A., Kong, Y., 2018. Comparison of secretome profile of pathogenic and non-pathogenic *Entamoeba histolytica*. Proteomics 18, e1700341.

Alsam, S., Sissons, J., Jayasekera, S., Khan, N.A., 2005. Extracellular proteases of *Acanthamoeba castellanii* (encephalitis isolate belonging to T1 genotype) contribute to increased permeability in an in vitro model of the human blood-brain barrier. J. Infect. 51, 150–156.

Amerik, A., Sindhi, N., Hochstrasser, M., 2006. A conserved late endosome-targeting signal required for Doa4 deubiquitylating enzyme function. J. Cell Biol. 175, 825–835.

Amerik, A.Y., Hochstrasser, M., 2004. Mechanism and function of deubiquitinating enzymes. Biochim. Biophys. Acta 1695, 189–207.

Behera, H.S., Satpathy, G., 2016. Characterisation and expression analysis of trophozoite and cyst proteins of *Acanthamoeba* spp. isolated from *Acanthamoeba* keratitis (AK) patient. Mol. Biochem. Parasitol. 205, 29–34.

Betanzos, A., Banuelos, C., Orozco, E., 2019. Host invasion by pathogenic amoebae: epithelial disruption by parasite proteins. Genes 10.

Broxton, C.N., Culotta, V.C., 2016. SOD enzymes and microbial pathogens: surviving the oxidative storm of infection. PLoS Pathog. 12, e1005295.

Cao, Z., Jefferson, D.M., Panjwani, N., 1998. Role of carbohydrate-mediated adherence in cytopathogenic mechanisms of *Acanthamoeba*. J. Biol. Chem. 273, 15838–15845.

Caumo, K.S., Monteiro, K.M., Ott, T.R., Maschio, V.J., Wagner, G., Ferreira, H.B., Rott, M. B., 2014. Proteomic profiling of the infective trophozoite stage of *Acanthamoeba polyphaga*. Acta Trop. 140, 166–172.

Clarke, D.W., Niederkorn, J.Y., 2006. The pathophysiology of *Acanthamoeba* keratitis. Trends Parasitol. 22, 175–180.

Coelho, C.H., Costa, A.O., Silva, A.C., Pucci, M.M., Serufo, A.V., Busatti, H.G., Durigan, M., Perales, J., Chapeaurouge, A., da Silva, E.S.D.A., Gomes, M.A., Toledo, J.S., Singer, S.M., Silva-Pereira, R.A., Fernandes, A.P., 2016. Genotyping and descriptive proteomics of a potential zoonotic canine strain of *Giardia duodenalis*, infective to mice. PloS One 11, e0164946.

Corsaro, D., Walochnik, J., Kohsler, M., Rott, M.B., 2015. *Acanthamoeba* misidentification and multiple labels: redefining genotypes T16, T19, and T20 and proposal for *Acanthamoeba micheli* sp. nov. (genotype T19). Parasitol. Res. 114, 2481–2490.

Costa, A.O., Furst, C., Rocha, L.O., Cirelli, C., Cardoso, C.N., Neiva, F.S., Possamai, C.O., de Assis Santos, D., Thomaz-Soccol, V., 2017. Molecular diagnosis of *Acanthamoeba* keratitis: evaluation in rat model and application in suspected human cases. Parasitol. Res. 116, 1339–1344.

Dirac, A.M., Nijman, S.M., Brummelkamp, T.R., Bernards, R., 2005. Functional annotation of deubiquitinating enzymes using RNA interference. Methods Enzymol. 398, 554–567.

Duarte, J.L., Furst, C., Klisiowicz, D.R., Klassen, G., Costa, A.O., 2013. Morphological, genotypic, and physiological characterization of *Acanthamoeba* isolates from keratitis patients and the domestic environment in Vitoria, Espirito Santo, Brazil. Exp. Parasitol. 135, 9–14.

el-Mezgueldi, M., 1996. Calponin. Int. J. Biochem. Cell Biol. 28, 1185–1189.

Fridovich, I., 1995. Superoxide radical and superoxide dismutases. Annu. Rev. Biochem. 64, 97–112.

Galkin, A., Kulakova, L., Melamud, E., Li, L., Wu, C., Mariano, P., Dunaway-Mariano, D., Nash, T.E., Herzberg, O., 2007. Characterization, kinetics, and crystal structures of fructose-1,6-bisphosphate aldolase from the human parasite, *Giardia lamblia*. J. Biol. Chem. 282, 4859–4867.

Garate, M., Marchant, J., Cubillos, I., Cao, Z., Khan, N.A., Panjwani, N., 2006. In vitro pathogenicity of *Acanthamoeba* is associated with the expression of the mannose-binding protein. Invest. Ophthalmol. Vis. Sci. 47, 1056–1062.

Garavaglia, P.A., Laverriere, M., Cannata, J.J., Garcia, G.A., 2016. Putative role of the aldo-keto reductase from *Trypanosoma cruzi* in benznidazole metabolism. Antimicrob. Agents Chemother. 60, 2664–2670.

Gonzalez-Robles, A., Castanon, G., Hernandez-Ramirez, V.I., Salazar-Villatoro, L., Gonzalez-Lazaro, M., Omana-Molina, M., Talamas-Rohana, P., Martinez-Palomo, A., 2008. *Acanthamoeba castellanii*: identification and distribution of actin cytoskeleton. Exp. Parasitol. 119, 411–417.

Guerin, J.L., Gelfi, J., Camus, C., Delverdier, M., Whisstock, J.C., Amardeihl, M.F., Py, R., Bertagnoli, S., Messud-Petit, F., 2001. Characterization and functional analysis of Serp3: a novel myxoma virus-encoded serpin involved in virulence. J. Gen. Virol. 82, 1407–1417.

Hong, Y.C., Lee, W.M., Kong, H.H., Jeong, H.J., Chung, D.I., 2004. Molecular cloning and characterization of a cDNA encoding a laminin-binding protein (AhLBP) from *Acanthamoeba healyi*. Exp. Parasitol. 106, 95–102.

Itoh, Y.a.M.S., 2002. Membrane-Type Matrix Metalloproteinases.

James, C.R.a., 1985. α1-Antitrypsin and the serpins: variation and countervariation. Trends Biochem. Sci. 4, 10–20.

Kalra, S.K., Sharma, P., Shyam, K., Tejan, N., Ghoshal, U., 2020. *Acanthamoeba* and its pathogenic role in granulomatous amebic encephalitis. Exp. Parasitol. 208, 107788.

Kim, W.T., Kong, H.H., Ha, Y.R., Hong, Y.C., Jeong, H.J., Yu, H.S., Chung, D.I., 2006. Comparison of specific activity and cytopathic effects of purified 33 kDa serine proteinase from *Acanthamoeba* strains with different degree of virulence. Kor. J. Parasitol. 44, 321–330.

Kong, H.H., Kim, T.H., Chung, D.I., 2000. Purification and characterization of a secretory serine proteinase of *Acanthamoeba healyi* isolated from GAE. J. Parasitol. 86, 12–17.

Lin, W.C., Wang, L.C., Pang, T.L., Chen, M.Y., 2015. Actin-binding protein G (AbpG) participates in modulating the actin cytoskeleton and cell migration in *Dictyostelium discoideum*. Mol. Biol. Cell 26, 1084–1097.

Lorenzo-Morales, J., Khan, N.A., Walochnik, J., 2015. An update on *Acanthamoeba* keratitis: diagnosis, pathogenesis and treatment. Parasite 22, 10.
Maciver, S.K., Asif, M., Simmen, M.W., Lorenzo-Morales, J., 2013. A systematic analysis of *Acanthamoeba* genotype frequency correlated with source and pathogenicity: T4 is confirmed as a pathogen-rich genotype. Eur. J. Protistol. 49, 217–221.
Maschio, V.J., Virginio, V.G., Ferreira, H.B., Rott, M.B., 2018. Comparative proteomic analysis of soluble and surface-enriched proteins from *Acanthamoeba* castellanii trophozoites. Mol. Biochem. Parasitol. 225, 47–53.
Mazur, T., Hadas, E., 1994. The effect of the passages of *Acanthamoeba* strains through mice tissues on their virulence and its biochemical markers. Parasitol. Res. 80, 431–434.
Michalek, M., Sonnichsen, F.D., Wechselberger, R., Dingley, A.J., Hung, C.W., Kopp, A., Wienk, H., Simanski, M., Herbst, R., Lorenzen, I., Marciano-Cabral, F., Gelhaus, C., Gutsmann, T., Tholey, A., Grotzinger, J., Leippe, M., 2013. Structure and function of a unique pore-forming protein from a pathogenic acanthamoeba. Nat. Chem. Biol. 9, 37–42.
Moon, K.B., Turner, P.C., Moyer, R.W., 1999. SPI-1-dependent host range of rabbitpox virus and complex formation with cathepsin G is associated with serpin motifs. J. Virol. 73, 8999–9010.
Neelam, S., Niederkorn, J.Y., 2017. Pathobiology and immunobiology of *Acanthamoeba* keratitis: insights from animal models. Yale J. Biol. Med. 90, 261–268.
Nijman, S.M., Luna-Vargas, M.P., Velds, A., Brummelkamp, T.R., Dirac, A.M., Sixma, T. K., Bernards, R., 2005. A genomic and functional inventory of deubiquitinating enzymes. Cell 123, 773–786.
Penning, T.M., 2015. The aldo-keto reductases (AKRs): Overview. Chem. Biol. Interact. 234, 236–246.
Ramirez-Rico, G., Martinez-Castillo, M., de la Garza, M., Shibayama, M., Serrano-Luna, J., 2015. *Acanthamoeba castellanii* proteases are capable of degrading iron-binding proteins as a possible mechanism of pathogenicity. J. Eukaryot. Microbiol. 62, 614–622.
Ren, M., Wu, X., 2010. Evaluation of three different methods to establish animal models of *Acanthamoeba* keratitis. Yonsei Med. J. 51, 121–127.
Siddiqui, R., Iqbal, J., Maugueret, M.J., Khan, N.A., 2012. The role of Src kinase in the biology and pathogenesis of *Acanthamoeba castellanii*. Parasites Vectors 5, 112.
Sissons, J., Alsam, S., Goldsworthy, G., Lightfoot, M., Jarroll, E.L., Khan, N.A., 2006. Identification and properties of proteases from an *Acanthamoeba* isolate capable of producing granulomatous encephalitis. BMC Microbiol. 6, 42.
Soto-Arredondo, K.J., Flores-Villavicencio, L.L., Serrano-Luna, J.J., Shibayama, M., Sabanero-Lopez, M., 2014. Biochemical and cellular mechanisms regulating *Acanthamoeba castellanii* adherence to host cells. Parasitology 141, 531–541.
Trochine, A., Alvarez, G., Corre, S., Faral-Tello, P., Duran, R., Batthyany, C.I., Cerecetto, H., Gonzalez, M., Robello, C., 2014. *Trypanosoma cruzi* chemical proteomics using immobilized benznidazole. Exp. Parasitol. 140, 33–38.
Verissimo, C.M., Maschio, V.J., Correa, A.P., Brandelli, A., Rott, M.B., 2013. Infection in a rat model reactivates attenuated virulence after long-term axenic culture of *Acanthamoeba* spp. Mem. Inst. Oswaldo Cruz 108, 832–835.
Visvesvara, G.S., Balamuth, W., 1975. Comparative studies on related free-living and pathogenic amebae with special reference to *Acanthamoeba*. J. Protozool. 22, 245–256.
Visvesvara, G.S., Moura, H., Schuster, F.L., 2007. Pathogenic and opportunistic free-living amoebae: *Acanthamoeba* spp., *Balamuthia mandrillaris*, *Naegleria fowleri*, and *Sappinia diploidea*. FEMS Immunol. Med. Microbiol. 50, 1–26.
Yang, Y.N., Bauer, D., Wasmuth, S., Steuhl, K.P., Heiligenhaus, A., 2003. Matrix metalloproteinases (MMP-2 and 9) and tissue inhibitors of matrix metalloproteinases (TIMP-1 and 2) during the course of experimental necrotizing herpetic keratitis. Exp. Eye Res. 77, 227–237.